THE JOURNAL OF BIOLOGICAL CHEMISTRY VOL. 287, NO. 53, pp. 44761–44771, December 28, 2012

Hypoxia-inducible Factor 1-α Induces miR-210 in Normoxic Differentiating Myoblasts*[S]

Received for publication, September 20, 2012, and in revised form, November 9, 2012 Published, JBC Papers in Press, November 12, 2012, DOI 10.1074/jbc.M112.421255

Lucia Cicchillitti[‡], Valeria Di Stefano[‡§], Eleonora Isaia[‡], Luca Crimaldi[‡1], Pasquale Fasanaro[§], Valeria Ambrosino[¶], Annalisa Antonini[§], Maurizio C. Capogrossi[§], Carlo Gaetano[‖], Giulia Piaggio[¶], and Fabio Martelli[‡2]

From the [‡]IRCCS-Policlinico San Donato, 20097 Milan, Italy, the [§]Istituto Dermopatico dell'Immacolata-IRCCS, 00167 Rome, Italy, the [¶]Istituto Nazionale dei Tumori Regina Elena, 00158 Rome, Italy, and the [‖]Uniklinikum-Goethe University, 60590 Frankfurt am Main, Germany

Background: miR-210 hypoxamir is induced by Hif1a in hypoxic cells.
Results: miR-210 expression increased during myogenic differentiation in normoxia with a Hif1a-dependent mechanism. Moreover, miR-210 displayed a cytoprotective role in response to mitochondrial dysfunction and oxidative stress.
Conclusion: miR-210 regulation and function extend beyond cell response to hypoxia.
Significance: Identifying miR-210 as a potential target in skeletal muscle disorders.

MicroRNA-210 (miR-210) induction is a virtually constant feature of the hypoxic response in both normal and transformed cells, regulating several key aspects of cardiovascular diseases and cancer. We found that miR-210 was induced in normoxic myoblasts upon myogenic differentiation both *in vitro* and *in vivo*. miR-210 transcription was activated in an hypoxia-inducible factor 1-α (Hif1a)-dependent manner, and chromatin immunoprecipitation experiments show that Hif1a bound to the miR-210 promoter only in differentiated myotubes. Accordingly, luciferase reporter assays demonstrated the functional relevance of the Hif1a binding site for miR-210 promoter activation in differentiating myoblasts. To investigate the functional relevance of increased miR-210 levels in differentiated myofibers, we blocked miR-210 with complementary locked nucleic acid oligonucleotides (anti-miR-210). We found that C2C12 myoblast cell line differentiation was largely unaffected by anti-miR-210. Likewise, miR-210 inhibition did not affect skeletal muscle regeneration following cardiotoxin damage. However, we found that miR-210 blockade greatly increased myotube sensitivity to oxidative stress and mitochondrial dysfunction. In conclusion, miR-210 is induced in normoxic myofibers, playing a cytoprotective role.

MicroRNA-210 (miR-210)[3] induction is a virtually constant feature of the hypoxic response in both normal and transformed cells, regulating several key aspects of health and disease (1–4). Indeed, miR-210 is a robust target of hypoxia-inducible factor (HIF). HIF1A isoform-specific induction has been reported in several cell types (5–9), albeit regulation by HIF2A was observed as well (10).

Given the wide impact of miR-210 on hypoxic cell metabolism, redox balance, survival, and angiogenesis, it has also been named as a master miRNA of the hypoxia response (hypoxamiR) (11). In keeping with its pleiotropic function, a broad spectrum of miR-210 targets has been identified (1, 2, 12).

Reduced survival of cells devoid of miR-210 in normoxia and/or hypoxia is well documented (7–9, 13–16). Moreover, miR-210 plays an instrumental role in the cytoprotection afforded to bone marrow-derived mesenchymal stem cells by ischemia/reoxygenation, supporting their survival under subsequently longer exposure to anoxia and following engraftment in the infarcted heart (17). Although the molecular mechanisms underpinning these events are complex, miR-210 directly represses the apoptotic component CASP8AP2 (17) as well as other apoptosis-related genes such as DAPK1 and, at least in humans, AIFM3 (14, 18, 19). However, miR-210 function seems to be complex and context-dependent because increased apoptosis upon miR-210 overexpression in normoxia has been reported as well (8, 9).

miR-210 also influences mitochondrial metabolism: By down-regulating the expression of iron-sulfur cluster scaffold protein ISCU1/2, miR-210 disrupts the mitochondrial electron transport activity, providing a mechanistic insight into the shift from mitochondrial respiration to glycolysis observed in hypoxia (8, 12, 20–22). Accordingly, miR-210 can also modulate the generation of reactive oxygen species (ROS) (8, 20, 22). Moreover, expression of miR-210 in human umbilical vein endothelial cells results in more tubulogenesis and increased VEGF-induced cell migration through the repression of the receptor tyrosine kinase ligand Ephrin-A3 (7, 23, 24). Confirming miR-210 proangiogenic role, up-regulation of miR-210 in CD34+ cells enhanced tissue perfusion and capillary density in a mouse model of hind limb ischemia (25).

In keeping with its hypoxamiR role, orchestrating cell and tissue response to ischemia, miR-210 expression is also increased during erythropoietin-induced erythroid differentiation, and miR-210 inhibition in this context leads to apoptosis

* This work was supported in part by Ministero della Salute and Associazione Italiana per la Ricerca sul Cancro Grant AIRC IG-11436.
[S] This article contains supplemental Figs. S1–S8 and Tables S1–S4.
[1] Present address: Istituto Europeo di Oncologia, Milan, Italy.
[2] To whom correspondence should be addressed: Molecular Cardiology Laboratory, IRCCS-Policlinico San Donato, via Morandi 30, San Donato Milanese, 20097 Milan, Italy. Tel.: 390252774533; Fax: 390252774666; E-mail: fabio.martelli@grupposandonato.it.
[3] The abbreviations used are: miR, microRNA; HIF, hypoxia-inducible factor; ROS, reactive oxygen species; DM, differentiation medium; GM, growing medium; DHE, dihydroethidium; LNA, locked nucleic acid; qPCR; quantitative PCR; CTX, cardiotoxin; HRE, Hypoxia Response Elements.

(13). Moreover, miR-210 might be involved in increased expression of γ-globin genes in differentiating erythroid cells (26).

miR-210 seems to have functions independent of its hypoxamiR role. miR-210 regulates normoxic gene expression involved in tumor initiation (5) and promotes both osteoblastic and adipocyte differentiation (27, 28).

Given the complexity of miR-210 action, it is not surprising that miR-210 is involved in several key aspects of health and disease. Indeed, miR-210 overexpression has been detected in a variety of cardiovascular diseases, including myocardial infarction, heart failure, and stroke, as well as in solid tumors, such as breast and pancreatic cancer (1, 2, 4, 29).

In this study, we found that miR-210 expression levels increased during myogenic differentiation, both *in vitro* and *in vivo*, and that this regulation occurred at the transcriptional level with a Hif1a-dependent mechanism. We also identified the Hif1a binding site responsible for the robust induction of the miR-210 promoter. Moreover, we demonstrated a pivotal cytoprotective role of miR-210 in response to mitochondrial dysfunction and oxidative stress.

EXPERIMENTAL PROCEDURES

Cell Culture—The mouse C2C12 myoblast cell line (ATCC) was cultured in DMEM containing 20% FCS as described previously (30). Differentiation was induced by plating the cells in DMEM containing 2% horse serum (differentiation medium, DM). Polyclonal populations of quail myoblasts transformed by the temperature-sensitive mutant of the Rous sarcoma virus LA29 were established and cultured as described (31). Briefly, the quail myoblast line was propagated at 35 °C in DMEM supplemented with 10% FCS and 10% tryptose phosphate broth (GM conditions). Differentiation was induced by plating the cells on collagen-coated dishes in GM and, the following day, incubating the cells with DMEM supplemented with 2% FCS at 41 °C (DM conditions). L6C5 rat myoblasts were maintained in DMEM supplemented with 15% FCS (GM). Differentiation was induced by plating the cells in DMEM containing 1% horse serum and 1 mg/ml of insulin (DM). To induce hypoxia, cells were cultured in a hypoxic incubator at 1% oxygen tension (Forma series II incubator, model no. 3131). For drug treatments, C2C12 cells were grown for 24 h in DM and then treated with either solvent alone or the following drugs: 200 μM H2O2, 40 mM NaN3, 2 μM Rotenone, and 6 μM antimycin A (all from Sigma-Aldrich).

Immunoblotting—Cells were lysed in 2× Laemmli buffer and boiled for 5 min. Equal amounts of proteins were separated by SDS-PAGE and transferred to nitrocellulose by standard procedures. Proteins of interest were detected with the following specific antibodies: anti-Hif1a (H1α6, Novus Biological), and anti-α-tubulin (Ab-1, Oncogene Research Product).

Indirect Immunofluorescence—Cells were fixed with 4% paraformaldehyde, and immunofluorescence staining was performed as described previously (32). Myotubes were identified using a myosin heavy chain, Myh2 antibody (MF 20 mouse hybridoma). Cells were counterstained with Hoechst 33342 (Sigma-Aldrich). Images were acquired by a fluorescence microscope (Axioplan 2, Carl Zeiss), analyzed by IAS software (Delta System). Myotubes and nuclei were counted by two blinded readers obtaining similar results. The fusion index was calculated as the percentage of nuclei belonging to myosin heavy chain-positive cells with three or more nuclei (33).

Oxidative Stress—Cell cultures were incubated at 37 °C with 2 μM dihydroethidium (DHE) (Sigma-Aldrich) or 5 μM MitoSOX (Molecular Probes, Invitrogen) for 15 min and 10 min, respectively. Then, cells were fixed with 4% paraformaldehyde, nuclei were stained with Hoechst 33342, and fluorescence was revealed by fluorescence microscopy using the same exposure conditions for each sample and quantified using Scion Image software as described previously (7). DHE and MitoSOX fluorescence was normalized for the number of Hoechst 33342-positive nuclei.

miRNA Down-modulation and RNAi—Locked nucleic acid (LNA) oligonucleotides against miR-210 (*in vivo* LNA miR-210 inhibitor) or a control scramble LNA sequence (40 nM, both from Exiqon) were transfected using siRNA transfection reagent (SC 29528, Santa Cruz Biotechnology) in C2C12 in GM. After 16 h, cells were washed, and fresh medium was added, and experiments were performed 24 h later.

For siRNA silencing, C2C12 cells were transfected with the HiPerfect transfection reagent (Qiagen) complexed with siRNAs according to the instructions of the manufacturer. Briefly, in C2C12 RNAi for a single molecule was performed by complexing 6 μl of HiPerfect and 25 nM siRNA targeting Hif1a (SC 35562, Santa Cruz Biotechnology) or a scramble sequence per 35-mm dish. After 16 h, cells were washed, and fresh medium was added.

For shRNA-mediated knockdown, the following shRNA pLKO.1 plasmids were employed: pLKO.1 empty (Addgene 8543), pLKO.1 scrambled shRNA (Addgene 1864), and pLKO.1 Hif1a shRNA (Sigma-Aldrich TRCN0000232220, TRCN-0000232222, and TRCN0000232223). Lentiviral generation and infection were performed as described previously (34). Uninfected cells were selected out by puromycin selection.

miRNA and mRNA Quantification—Total RNA was extracted using TRIzol (Invitrogen). miRNA levels were analyzed using the Applied Biosystems TaqMan quantitative real-time PCR method (qPCR, 1 ng/assay) performed according to the instructions of the manufacturer and quantified with the ABI Prism 7000 SDS (Applied Biosystems). Mature miRNA levels were normalized to miR-16, whereas pri-miR-210 levels were normalized to GAPDH.

Hif1a mRNA Levels Were Analyzed Using Applied Biosystems TaqMan Quantitative Real-time PCR Method (1 ng/assay)—mRNAs levels were analyzed using the SYBR-Green qPCR method (5 ng/assay, Qiagen) performed according to the instructions of the manufacturer using supplemental Table S1 primers and quantified with ABI Prism 7000 SDS (Applied Biosystems). mRNA expression was normalized for β-2-microglobulin (B2m) or Rpl13 levels. For both miRNAs and mRNAs, relative expression was calculated using the comparative Ct method ($2^{--\Delta\Delta Ct}$).

ChIP Assay—The procedure for ChIP was performed as described previously (35). Briefly, 1% formaldehyde was added directly to the cells and incubated at 22 °C for 10 min. The reaction was stopped adding 0.125 M glycine. Then, the cells

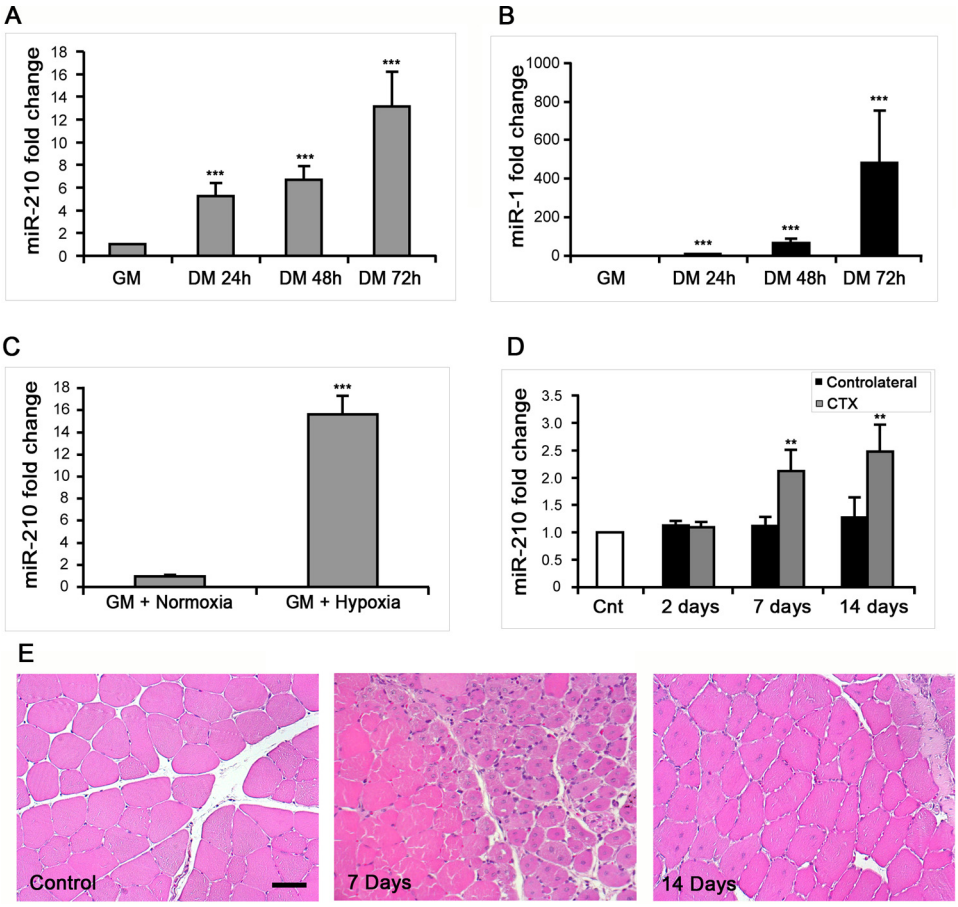

FIGURE 1. **Positive modulation of miR-210 upon myogenic differentiation.** C2C12 cells were cultured in GM and then switched to DM for the indicated period of time. Then, RNA was extracted, and miR-210 (*A*) and miR-1 (*B*, positive control) levels were measured by qPCR ($n = 25$; ***, $p < 0.001$). *C*, C2C12 myoblasts were cultured in GM and exposed to 1% oxygen tension for 48 h. miR-210 levels were measured in normoxic and hypoxic cells by qPCR ($n = 6$; ***, $p < 0.001$). *D* and *E*, tibialis anterior muscles were injected with CTX to induce skeletal muscle fiber selective damage followed by regeneration. 7 and 14 days later, RNA was extracted, and miR-210 was measured (*D*). Increased miR-210 levels correlated with myogenic regeneration. *E*, representative H&E-stained sections. Small, centrally nucleated myofibers are present both 7 and 14 days after CTX injection. *Scale bar* = 50 μM.

were rinsed with cold 1× PBS, incubated with 0.2× trypsin-EDTA in 1× PBS, and scraped. cells were centrifuged, washed in cold 1× PBS plus 0.5 mM PMSF and resuspended in lysis buffer (5 mM piperazine N,N bis zethone sulfonic acid (pH 8.85) mM KCl, 0.5% Nonidet P-40). Next, nuclei were solicited in the sonication buffer (0.1% SDS, 10 mM EDTA, 50 mM Tris-HCl (pH 8), 0.5% deoxycholic acid) for 10 min by using a microultrasonic cell disruptor. The chromatin was sheared to an average size of 500 base pairs, and immunoprecipitation was performed with protein G-agarose (KPL). The chromatin solution was precleared by adding protein G for 1 h at 4 °C and incubated at 4 °C overnight with 4 μg of Hif1a antibody (H1α6, Novus Biological) or non-specific immunoglobulins (IgGs, Santa Cruz Biotechnology) as negative control. Input was collected from a control sample supernatant (not immunoprecipitated antibody). Immunoprecipitates were recovered by incubation for 2 h at 4 °C with protein G-agarose precleared previously in immunoprecipitation buffer (1 μg/μl bovine serum albumin, 1 μg/μl salmon testis DNA, protease inhibitors, and PMSF). Reversal of formaldehyde cross-linking, RNase A, and proteinase K treatments were performed as described previously (35). DNA was phenol-extracted, ethanol-precipitated, and analyzed by PCR. DNA representing 0.005–0.01% of the total chromatin sample (input) or 1–10% of the immunoprecipitates was amplified using specific primers indicated in supplemental Table S2.

Reporter Assay—miR-210 promoter constructs were generated using pGL2 firefly luciferase vector (Promega) adopting standard techniques. Relevant mouse genomic DNA fragments were amplified using supplemental Table S3 primers and cloned between the BglII and HindIII sites. For the HRE mutational analysis, HRE 1 and 2 were mutated within the D construct promoter sequence either alone (D mut 1 and D mut 2) or in combination (D mut 1 + 2). The HREs (A/GCGTG) were mutated to A/GAAAG. The corresponding DNA fragments were obtained from the Integrated DNA Technologies (IDT) gene synthesis service (TEMA ricerca) and then subcloned in the pGL2 luciferase plasmid. pGL2 luciferase plasmids were cotransfected with a pRL-null plasmid encoding *Renilla* luciferase (Promega). All transfections were carried out using FuGENE 6 transfection reagent (Roche), and luciferase activity was measured using the dual luciferase assay system (Promega) according to the instructions of the manufacturers.

Analysis of miR-210 CpG Island Methylation—To identify CpG islands in the 2.373 kb upstream mature miR-210, the DNA sequence was submitted to the CpG Island Searcher using the following parameters: length, 300 bp; ObsCpG/ExpCpG,

70%; and %GC, 60%. C2C12 DNA bisulfite conversion was performed directly using the EZ DNA Methylation-Direct kit following the recommendations of the manufacturer (Zymo Research). Products of the bisulfite reactions were PCR-amplified using the HotMaster TaqDNA polymerase kit (5 PRIME) using supplemental Table S4 primers. The products were resolved on a 1.6% agarose gel, purified using a MinElute gel extraction kit (Qiagen), subcloned into the pDRIVE vector (using a Qiagen PCR cloning kit), and sequenced.

Mouse Model of Skeletal Muscle Regeneration—All experimental procedures complied with the guidelines of the Italian National Institutes of Health and with the Guide for the Care and Use of Laboratory Animals (Institute of Laboratory Animal Resources, National Academy of Sciences, Bethesda, MD) and were approved by the institutional Animal Care and Use Committee. Two-month-old CD1 male mice were used. *In vivo* down-modulation of miR-210 was carried out by tail vein injection of 12 mg/kg "*in vivo* LNA miR-210 inhibitor" (Exiqon) or an LNA scrambled sequence (SCR). For longer time courses, a second LNA oligonucleotide dose was administered at day 7. Two days after the first LNA administration, tibialis anterior muscle injury was induced by cardiotoxin (CTX, Calbiochem) injection as described previously (32). Next, both treated and controlateral muscles were harvested and split into two parts. Half was fixed, paraffin-embedded, and used for histological analysis. The other half was used for RNA extraction. To measure CDX-induced damage, myofiber permeability was measured by intraperitoneal injection of Evans Blue dye (Sigma-Aldrich) 16 h before sacrifice, as described previously (36). Thereafter, muscles were harvested and split into two parts. Half was frozen in OCT embedding medium, and half was used for RNA extraction.

Histology and Morphometric Analysis—H&E sections of paraffin-embedded muscles were prepared as described previously (32), and regenerating centrally nucleated myofibers were counted. Frozen sections of Evans Blue dye-stained muscles were fixed in cold acetone at −20 °C for 10 min, washed in PBS, and mounted with fluorescence mounting medium. A Zeiss Axioplan 2 fluorescence microscope with image analyzer KS300 software was used to acquire images and to measure areas. All histological and morphometric analyses were carried out by two blinded readers with comparable results.

Statistical Analysis—Variables were analyzed by both Student's *t* test and one-way analysis of variance, and $p \leq 0.05$ was deemed statistically significant. Values are expressed as mean ± S.E.

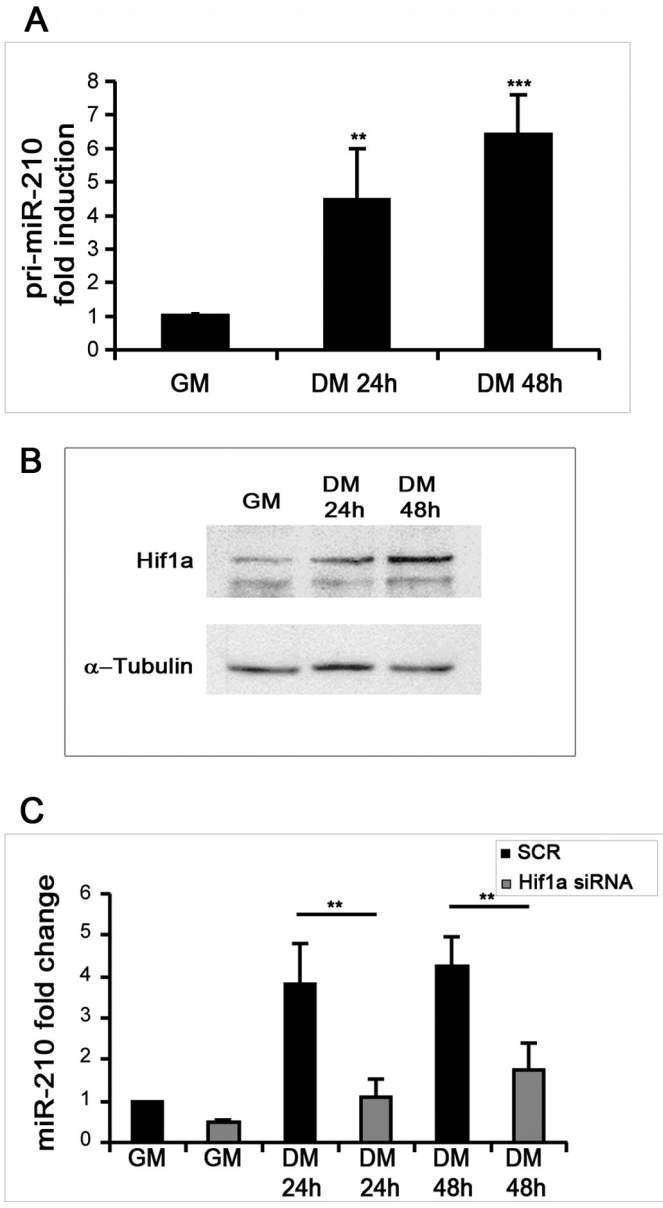

FIGURE 2. **miR-210 transcriptional activation upon myogenic differentiation is Hif1a-dependent.** C2C12 cells were cultured in GM and then switched to DM for the indicated time. *A*, RNA was extracted, and pri-miR-210 levels were measured by qPCR. Pri-miR-210 was induced during differentiation ($n = 5$; ** $p < 0.01$; *** $p < 0.001$). *B*, alternatively, protein extracts were derived, and Hif1a protein levels were measured by Western blot analysis. α-tubulin levels were used for gel loading control. Hif1a protein increased during C2C12 differentiation. *C*, C2C12 cells were transfected with a Hif1a-specific siRNA (*Hif1a siRNA*) or with a control scramble sequence (*SCR*). Then, cells were allowed to differentiate in DM for the indicated time, and miR-210 levels were measured. Hif1a silencing significantly decreased miR-210 levels ($n = 9$; ** $p < 0.01$).

RESULTS

miR-210 Expression Is Enhanced during Myogenic Differentiation—To test whether miR-210 is modulated upon myogenic differentiation, we used the C2C12 mouse myoblast cell line, a widely accepted myogenesis model. C2C12 cells were cultured in GM and then switched to DM for 24, 48, and 72 h. When miR-210 levels were measured, we found that miR-210 expression increased during myogenic differentiation (Fig. 1*A*). As expected, muscle-specific miR-1 levels increased steadily during differentiation as well (Fig. 1*B*). As a comparison, miR-210 levels after 72 h in DM were similar to these observed when GM cultures of C2C12 were exposed to hypoxia for 48 h (Fig. 1*C*). miR-210 increase following muscle differentiation was not limited to C2C12 because miR-210 was similarly induced in independent myogenesis cell models, such as the rat myoblasts L6C5 (supplemental Fig. S1A) and quail myoblast cell lines (supplemental Fig. S1C). Again, a positive control was represented by increased miR-1 levels (supplemental Fig. S1, *B* and *D*).

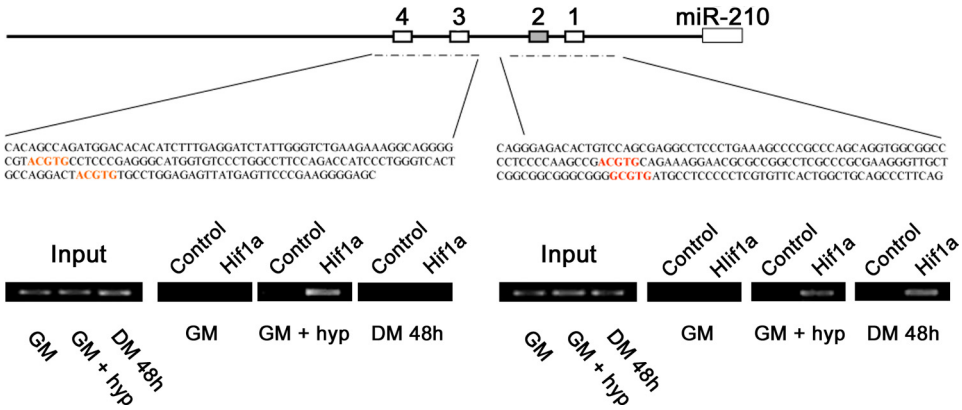

FIGURE 3. **ChIP analysis of the miR-210 promoter.** *Upper panel*, schematic representation of the HREs located in the ≈2.4-kbase promoter region upstream the mature miR-210. HRE 1, 2, 3, and 4 are located 437 bp, 495 bp, 841 bp, and 905 bp upstream of the mature miR-210, respectively. PCR was performed with primers specific to amplify promoter fragments containing the proximal two HREs (1 and 2) or the more distal HREs (3 and 4). The genomic sequence corresponding to the amplified fragments is displayed. The *lower panel* shows the Hif1a ChIP results. A ChIP analysis was performed using C2C12 cells cultured under GM or DM in normoxia for 48 h or GM and 1% oxygen tension for 24 h. *IgG* refers to samples derived for the IP negative control. In differentiated normoxic myotubes, Hif1a specifically bound only to the proximal fragment (HRE 1 and 2), whereas under hypoxia, Hif1a bound to both fragments.

Next, we investigated whether miR-210 was also induced during myogenesis *in vivo*. To this aim, myonecrosis was induced by CTX injection of tibialis anterior muscles. In Fig. 1, *D* and *E*, the time course experiment showed that at both days 7 and 14 after injection, skeletal muscle regeneration was associated with increased miR-210 levels. These data suggest that miR-210 up-regulation during myogenesis is likely functionally relevant.

miR-210 Induction during Differentiation Occurs at the Transcriptional Level and Is Hif1a-dependent—We sought to determine how miR-210 is regulated during differentiation. Fig. 2*A* shows that pri-miR-210 was induced upon myogenic differentiation to levels similar to these of the corresponding mature miRNA, indicating a transcriptional regulation of miR-210 during differentiation. These data were also confirmed with an independent primer couple (not shown). Next, given the importance of HIF1A for both miR-210 induction following hypoxia (1) and skeletal muscle physiopathology (37–40), we tested whether Hif1a silencing affected miR-210 induction in differentiating C2C12 cells.

Western blot analysis showed that Hif1a protein increased upon C2C12 differentiation (Fig. 2*B*). Next we assayed the effect of Hif1a silencing on miR-210 levels in differentiating myoblasts. The Hif1a transcript was not modulated during C2C12 differentiation and was significantly knocked down following specific siRNA transfection (supplemental Fig. S2). When miR-210 expression was measured, we found that miR-210 levels were decreased significantly at both the 24 and 48 h differentiation time points in Hif1a-silenced cells (Fig. 2*C*). miR-210 expression was decreased in myoblasts as well, but the difference did not reach statistical significance. Decreased miR-210 levels in DM were not simply due to an impairment of the differentiation process because the expression of myogenic markers such as miR-1, myogenin, and myosin heavy chain was unaffected (supplemental Fig. S2).

To confirm these findings, Hif1a was also knocked down in transducing C2C12 cells with a lentiviral vector expressing a specific shRNA (supplemental Fig. S3A). The adopted vector also carried a puromycin resistance gene, allowing the selection of infected cells. As expected, Hif1a silencing decreased miR-210 levels in hypoxic myoblasts (supplemental Fig. S3*B*). When normoxic differentiating myoblasts were measured, we found that miR-210 levels were decreased significantly by Hif1a shRNA both in GM and in DM. Indeed, after 48 h of differentiation, miR-210 levels were still lower than these observed in myoblasts expressing a scrambled control (supplemental Fig. S3*C*). This stronger inhibition of miR-210 expression was likely due to the higher efficiency of transduction yielded by infection followed by puromycin selection compared with transient transfection. Again, unaffected miR-1 induction upon differentiation indicated that myogenic differentiation was not grossly inhibited by Hif1a knockdown (supplemental Fig. S3*D*). These findings were further confirmed by two independent shRNA-targeting Hif1a (not shown).

Hif1a Binds to miR-210 Promoter, Activating Its Expression in Differentiating Myoblasts—Analysis of the ≈2.4 kbase promoter sequence upstream of the mature miR-210 sequence identified four potential HRE sites. To elucidate whether these sites were functionally relevant, a chromatin immunoprecipitation experiment was performed. As shown in Fig. 3, Hif1a antibody (but not control IgGs) immunoprecipitated the miR-210 promoter fragments in hypoxic and in differentiated C2C12 cells but very little in the normoxic undifferentiated controls. Specifically, two primer couples were used, encompassing the two proximal HRE (HRE1 and 2) and the two distal sites (HRE3 and 4). A more defined analysis was precluded by the close proximity of the HREs. We found that, although Hif1a bound to both fragments upon hypoxia, in differentiated myotubes Hif1a preferentially bound to the proximal fragment.

To better identify and characterize the functional HRE, we amplified ≈2.4 kbases of the genomic regions upstream of miR-210 sequence and generated serial deletion constructs (Fig. 4*A*). The promoter fragments were cloned into a luciferase vector, and the effect of the deletions on reporter gene activity during C2C12 myogenic differentiation was analyzed. Luciferase assays showed that the miR-210 promoter was induced in DM and that a 565-base fragment (D construct) that harbors the two proximal HRE sites (HRE1 and 2) was essential for sus-

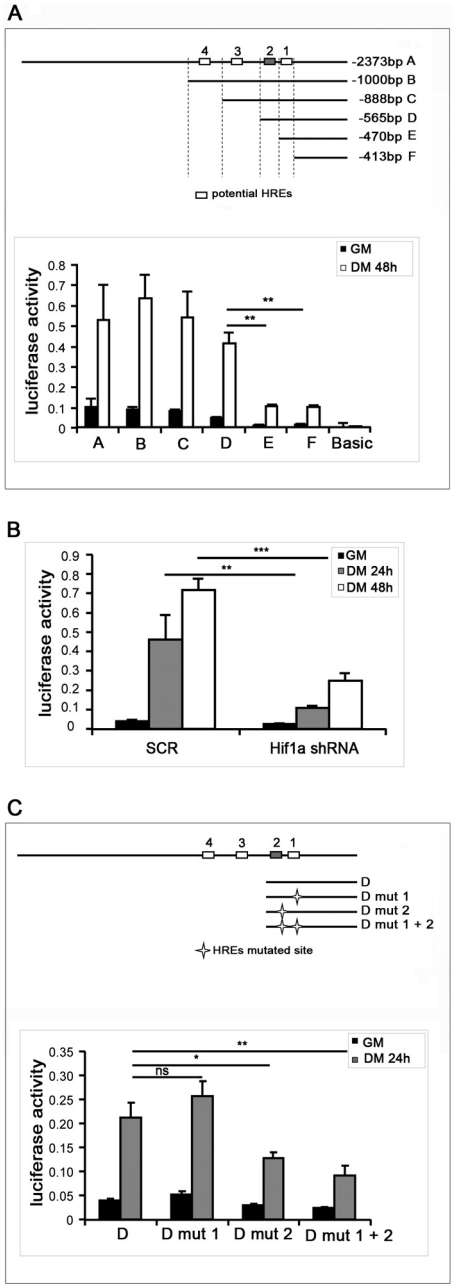

FIGURE 4. **Hif1a positively modulates miR-210 promoter activity during differentiation.** *A*, miR-210 promoter fragments were cloned into the pGL2-luciferase vector. Serial deletion constructs (identified by the letters *A–F*) are schematically represented above the *bar graph*. Predicted HREs are shown. *Lower panel*, the relative promoter activities in GM and DM 24 h are displayed. The empty pGL2-basic vector was used to monitor basal activity of the luciferase reporter gene (*Basic*). Luciferase activity is expressed as firefly/*Renilla* luciferase ratio. Constructs *A–D* displayed similar expression levels in DM, and activity dropped significantly in the *E* and *F* constructs ($n = 4$; $^{**}p < 0.01$). *B*, C2C12 cells infected with lentiviral vectors expressing either a Hif1a-specific shRNA (*Hif1a shRNA*) or a scramble (*SCR*) sequence were transfected with construct *D* (miR-210 565-bp promoter), and luciferase assays were performed in GM and in DM both at 24 and 48 h. D construct activity was significantly decreased in C2C12 myotubes when Hif1a was silenced ($n = 3$; $^{**}p < 0.01$; $^{***}p < 0.001$). *C*, *upper panel*, the two proximal HREs were mutated either alone (*D mut 1* and *D mut 2*) or in combination (*D mut 1+2*). *Lower panel*, promoter activity was detected by luciferase assays in C2C12 cells in GM and DM after 24 h. HRE2 mutation significantly decreased D construct activity, whereas HRE1 mutation was ineffective ($n = 6$; *, $p < 0.05$; **, $p < 0.01$; *ns*, not significant).

tained luciferase activity in differentiated myotubes (Fig. 4*A*). We also found that miR-210 D construct activity was decreased significantly in C2C12 myotubes where Hif1a was silenced, further corroborating the Hif1a role in miR-210 promoter modulation (Fig. 4*B*). Further deletions encompassing HRE2 (construct E) significantly decreased miR-210 promoter activity, although some residual functionality and inducibility were present (Fig. 4*A*). Interestingly, a similar pattern was observed when Hif1a overexpressing myoblasts were assayed, indicating that HRE1 was not functional (supplemental Fig. S4*A*). To confirm these findings, HRE1 and HRE2 were mutated, either alone or in combination. Fig. 4*C* shows that HRE2 mutation decreased the activity of the D construct, whereas HRE1 mutation was ineffective. Again, similar results were obtained when hypoxic myoblasts were assayed, although promoter activity was much stronger (supplemental Fig. S4*B*).

Finally, promoter analysis indicated the presence of a potential Myod binding site 523 nucleotides upstream of miR-210. However, mutational analysis showed that this sequence did not affect miR-210 promoter expression either in GM or in DM (supplemental Fig. S4*C* and Table S3).

Bioinformatic analysis of the ≈2.4 kbases upstream of the miR-210 mature sequence also indicated a potential CpG island from base −548 to base −280 (supplemental Fig. S4*D*), suggesting that DNA methylation may contribute to miR-210 promoter regulation during muscle differentiation. Indeed, a CpG island has been identified upstream of human miR-210 as well (41). When the cytosine methylation of this CpG-rich region was analyzed using the bisulfite technique, we found that methylation was almost undetectable in myoblasts and that the methylation status did not change during differentiation (not shown). In keeping with these findings, C2C12 treatment with 5-azacytidine demethylating drug for 24–72 h did not affect miR-210 expression (not shown). Thus, cytosine methylation does not seem to play a major role in miR-210 regulation during myogenic differentiation.

miR-210 Blockade Does Not Affect Myogenic Differentiation—To assess the functional role of miR-210 in skeletal muscle differentiation, we inhibited miR-210 in C2C12 cells using a LNA-modified antisense oligonucleotide (anti-miR-210). Although miR-210 levels were decreased more than 10-fold in differentiated cells (supplemental Fig. S5), we did not observe any overt alteration in myotube morphology (Fig. 5*A*, *left panel*). In keeping with this observation, the expression levels of myogenesis markers such as myogenin, desmin, myod, miR-1, miR-133a, and miR-133b were unaffected by miR-210 blockade (supplemental Fig. S5). Also, the myotube number (not shown), fusion index, and average number of nuclei per myotube after 48 h of differentiation did not change significantly (supplemental Fig. S6).

We also assayed whether miR-210 blockade *in vivo* affected skeletal muscle regeneration. miR-210 was inhibited by systemic anti-miR-210 administration, decreasing miR-210 levels > 10-fold (supplemental Fig. S7*A*). Skeletal muscle injury was induced by CTX injection, and Evans Blue staining showed that similar damage was induced in the two groups (supplemental Fig. S7*B*). Skeletal muscle regeneration was assayed 7 and 14 days after CTX injection. Although miR-210 was

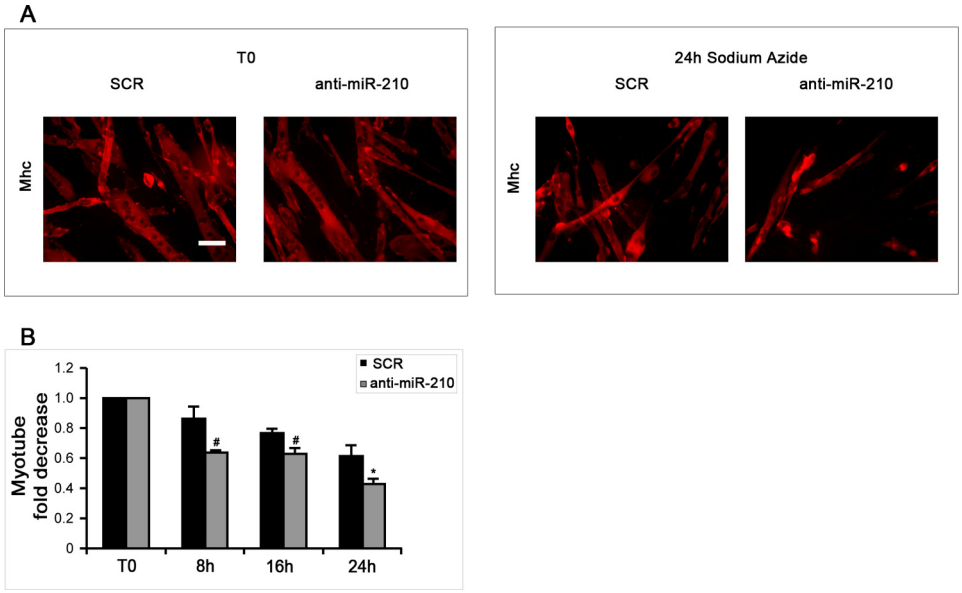

FIGURE 5. **miR-210 increases myotube survival under chemical anoxia induced by sodium azide treatment.** C2C12 myoblasts transfected with anti-miR-210 or a LNA control scramble sequence (*SCR*) were cultured for 24 h in DM and then treated with 40 mM sodium azide (NaN_3) for the indicated time to induce chemical anoxia. Next, cells were fixed and stained with MHC antibody, and the number of myotubes was counted. *A*, representative MHC immunofluorescence. *Scale bar* = 30 μM. *B*, *bar graph* showing a more pronounced NaN_3 toxicity in anti-miR-210 treated cultures ($n = 3$; * $p < 0.05$; #, $p < 0.02$).

decreased efficiently, the number of centrally nucleated regenerating myofibers was similar in anti-miR-210 and LNA-scrambled groups (supplemental Fig. S7*C*). In keeping with this finding, regeneration markers such as miR-206 and myogenin were induced similarly in the two groups both at days 7 and 14 (supplemental Fig. S7*D*). In conclusion, at least in the adopted experimental conditions, we found no evidence that miR-210 is necessary for myogenic differentiation.

miR-210 Increases Myotube Survival in the Presence of Mitochondrial Dysfunction and Oxidative Stress—During an intense skeletal muscle workload, the oxygen supply may not match the metabolic needs. This mismatch between oxygen supply and its demand at the cellular level may result in a hypoxic condition. miR-210 is induced by hypoxia, contributing to the adaptive mechanisms allowing cell survival. Although miR-210 induction by low oxygen tension is rapid, we asked whether high miR-210 levels observed in differentiated myotubes may boost cell survival, allowing a faster response. To evaluate the role of miR-210 when mitochondrial function is impaired, we blocked the electron transport chain by sodium azide, antimycin A, and rotenone (42). Although many differences exist, these drugs inhibit mitochondrial function, modeling insufficient oxygen supply, without the confounding effect of miR-210 induction (not shown). We found that sodium azide (Fig. 5), antimycin A (supplemental Fig. S8, *A* and *B*), and rotenone (supplemental Fig. S8, *C* and *D*) all decreased myotube survival as expected. However, the myotube number further decreased when miR-210 was inhibited.

One of the consequences of mitochondrial electron transport chain uncoupling is an increase of ROS production (43). Given the role of miR-210 in mitochondrial metabolism (1), we assayed whether miR-210 blockade increased C2C12 myotube levels of oxidative stress. miR-210 was inhibited by anti-miR-210 transfection, and oxidative stress was measured using DHE and MitoSOX fluorescent dyes, which are particularly sensitive to intracellular and mitochondrial superoxide anion levels, respectively. We found that both DHE- (Fig. 6, *A* and *B*) and MitoSOX- (*C* and *D*) associated fluorescence was increased significantly when miR-210 was blocked. Next, we assayed whether miR-210 levels affected myotube resistance to oxidative stress. After anti-miR-210 and LNA-scrambled transfection, C2C12 cells were allowed to differentiate for 48 h and were then challenged with a 200 μM H_2O_2 bolus. We found that myotube survival was further decreased when miR-210 was blocked (Fig. 6, *E* and *F*). We conclude that high levels of miR-210 in differentiated skeletal muscle contribute to the maintenance of the redox balance and to cell survival in the presence of mitochondrial and oxidative stresses.

DISCUSSION

miR-210 has been studied mostly for its role in cell and tissue response to hypoxia. Here we demonstrated that miR-210 is induced during normoxic myogenesis in different cell culture models. The relevance of these findings confirmed that miR-210 levels increased in regenerating skeletal muscles. We adopted the CTX model for this experiment because this drug targets muscle cells specifically, whereas vascular cells are largely unaffected (44). Thus, miR-210 levels were not increased by hypoxia because of a lack of perfusion. Accordingly, we observed that CTX treatment did not induce miR-210 acutely and that miR-210 levels increased only in the presence of concomitant muscle regeneration.

miR-210 is involved in other differentiating systems as well, independently of its hypoxamiR role. miR-210 promotes osteoblastic differentiation by inhibiting the expression of a type 1B receptor of activin A (AcvR1b) (27), and miR-210 also stimulates adipogenesis by repressing WNT signaling through targeting Tcf7l2 (28). Moreover, although its function in these systems is not yet known, miR-210 is also induced during epithelial cell and keratinocyte differentiation (45, 46) as well as in

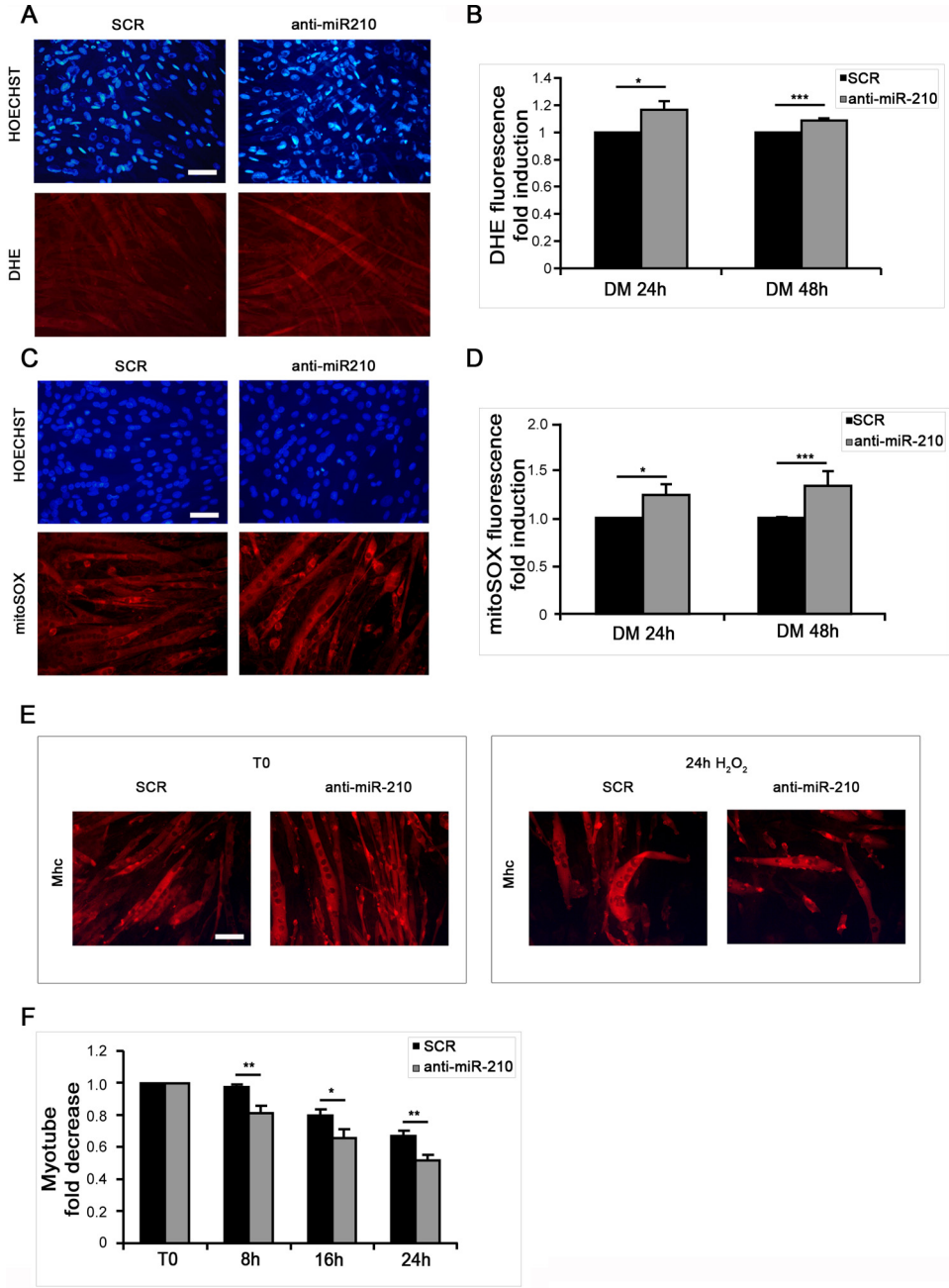

FIGURE 6. **miR-210 blockade significantly enhances ROS production in differentiated skeletal muscle cells.** C2C12 myoblasts transfected with anti-miR-210 or a LNA control scramble sequence (*SCR*) were allowed to differentiate for 24 h and 48 h in DM. Then, cells were treated with 2 μM DHE or 5 μM MitoSOX reagent for 15 min and 10 min, respectively, to measure oxidative stress. Nuclei were stained with Hoechst 33342, and fluorescence was revealed by fluorescence microscopy. Representative pictures display DHE (*A*) and MitoSOX (*C*) fluorescence. The *bar graphs* indicate DHE (*B*) and MitoSOX (*D*) fluorescence normalized for the number of Hoechst 33342-positive nuclei ($n = 3$; *, $p < 0.05$; ***, $p < 0.001$). C2C12 cells transfected with anti-miR-210 or SCR were cultured in DM for 24 h and then treated with 200 μM H_2O_2 for the indicated period of time. Myotube formation was detected by MHC immunofluorescence staining (*E*), and myotubes were counted (*F*). Result shows that myotube survival upon H_2O_2 treatment is further decreased when miR-210 is blocked ($n = 3$; *, $p < 0.05$; **, $p < 0.01$). *Scale bar* = 30 μM.

embryonic stem cells differentiating toward the endothelial lineage (47).

The induction of the miR-210 precursor (pri-miR-210) in differentiating myoblasts showed that its regulation occurred at the transcriptional level. We characterized the promoter region involved in this modulation, showing that Hif1a is a major player in the robust induction of the miR-210 promoter during C2C12 myogenic differentiation. We also identified a functional HRE site, localized at −495bp from mature mouse miR-210. Interestingly, this HRE site is localized in a genomic region highly conserved across species. Indeed, the 45-bp-encompassing mouse HRE2 displays 89% identity with the human miR-210 promoter sequence containing an HRE that Huang *et al.* (5) showed to be important for miR-210 induction upon hypoxia. Thus, these two binding sites are likely homologs. The mutation of the mouse HRE2 site greatly diminished promoter activity both during myogenic differentiation and hypoxia. In keeping with these data, Hif1a knockdown was associated with a

significant down-modulation of miR-210 levels and promoter activity, supporting the importance of Hif1a in the regulation of miR-210 expression in normoxic myofibers.

We also noticed that although Hif1a knockdown greatly decreased miR-210 promoter activity upon myogenic differentiation, some residual activity was present. Further investigations are needed to explore additional regulators of miR-210 expression during myogenesis. However, it is worth noting that Akt increases miR-210 levels through a Hif-independent mechanism in hypoxic cardiomyocytes (19), suggesting that a similar mechanism may be at work in skeletal muscles. Among the potential miR-210 regulators, a conserved NF-κB binding site has also been mapped in the 200-bp proximal promoter region (48). However, because myogenic differentiation correlates with loss of NF-κB transactivation function, it was not explored further (49). Finally, in most cell types, upon exposure to hypoxia, miR-210 is activated by HIF1A but not by HIF2A (5–9). Thus, we speculate that the same HIF isoform selection may likely be in place in differentiating myogenic cells. Nonetheless, Hif2a in normoxic myotubes cannot be ruled out.

Although Hif1a has been mainly characterized for its role in hypoxia response, Hif1a involvement in normoxic skeletal muscle physiology is not without precedent. Indeed, contrary to most tissues, it has been shown that Hif1a is present under normoxic conditions in a few mouse tissues, including skeletal muscle (39), where its level increases in response to systemic hypoxia (40) or ischemia (50).

Targeted deletion of Hif1a in mouse skeletal muscle affects exercise-induced gene regulatory responses of glycolytic enzymes. Skeletal muscle devoid of Hif1a also displays an increase in the activity of mitochondrial rate-limiting enzymes and the formation of excessive mitochondrial ROS. Conversely, development is largely unaffected (38). We found that Hif1a knockdown did not impair myogenic differentiation but blunted miR-210 expression. That, in turn, is a demonstrated modulator of mitochondrial metabolism and of intracellular ROS production (1). However, contrary to us, Ono *et al.* found that Hif1a knockdown had a negative impact on myoblast differentiation (37), possibly because of differences in the adopted experimental conditions.

To explore the functional role of increased miR-210 levels in differentiated myofibers, miR-210 was inhibited both *in vitro* and *in vivo*. Although several features of myogenic differentiation were measured, we failed to show that decreased miR-210 activity impairs myogenic differentiation significantly. However, it is possible that the effects of miR-210 blockade are subtle and that the adopted experimental conditions are inadequate to make them evident. Conversely, we found that miR-210 impairment affected myotube survival and oxidative stress levels. Myofibers, and in particular type I ones, mostly rely on oxidative metabolism, efficiently deriving ATP from glucose to match the intense energy consumption associated with muscle contraction. Oxidative metabolism, however, comes with a price, represented by ROS production by mitochondria (51). Paradoxically, ROS production is particularly significant in hypoxic conditions, when electron transport chain is uncoupled (43, 52). The workload type also seems to be important, with eccentric contractions inducing greater oxidative stress than concentric contractions (53).

Skeletal muscle is particularly prone to hypoxia and oxidative damage because during an intense workload, the oxygen supply may not match the need. In this respect, increased miR-210 levels seem to be instrumental to increase myofiber survival under metabolic stress conditions. Although many differences apply, it may be considered as a sort of "constitutive preconditioning," protecting metabolically active myofibers from mitochondrial dysfunction and oxidative stress. In keeping with this model, Kim *et al.* (17) demonstrated a crucial role of miR-210 in ischemia-reperfusion preconditioning. Furthermore, miR-210 inhibition increased oxidative stress levels of normoxic differentiated myoblasts, as observed previously in cardiac myocytes (19) and in hypoxic endothelial cells (20). Likewise, miR-210 also displayed a cytoprotective role in hypoxic cardiomyocytes (19). It is also worth noting that the magnitude of myofiber cytoprotection found in our studies was relatively modest, although similar to that found by others (18, 19).

In conclusion, we found that Hif1a induces miR-210 in normoxic differentiating myoblasts by direct transactivation of its promoter. The miR-210 cytoprotective role indicates future potential therapeutic applications in skeletal muscle ischemic and non-ischemic diseases. In this respect, preclinical evidence indicating miR-210 as a novel therapy for treatment of ischemic heart disease (18) is particularly encouraging.

Acknowledgments—We thank Dr. Germana Falcone (Consiglio Nazionale delle Ricerche, Rome, Italy) for quail myoblasts and L6C5 rat myoblasts. We also thank Prof. Antonio Musarò (Università Sapienza, Rome, Italy) for help with CTX experiments.

REFERENCES

1. Devlin, C., Greco, S., Martelli, F., and Ivan, M. (2011) miR-210. More than a silent player in hypoxia. *IUBMB Life* **63,** 94–100
2. Huang, X., Le, Q. T., and Giaccia, A. J. (2010) MiR-210-micromanager of the hypoxia pathway. *Trends Mol. Med.* **16,** 230–237
3. Voellenkle, C., van Rooij, J., Guffanti, A., Brini, E., Fasanaro, P., Isaia, E., Croft, L., David, M., Capogrossi, M. C., Moles, A., Felsani, A., and Martelli, F. (2012) Deep-sequencing of endothelial cells exposed to hypoxia reveals the complexity of known and novel microRNAs. *RNA* **18,** 472–484
4. Ivan, M., Harris, A. L., Martelli, F., and Kulshreshtha, R. (2008) Hypoxia response and microRNAs. No longer two separate worlds. *J. Cell Mol. Med.* **12,** 1426–1431
5. Huang, X., Ding, L., Bennewith, K. L., Tong, R. T., Welford, S. M., Ang, K. K., Story, M., Le, Q. T., and Giaccia, A. J. (2009) Hypoxia-inducible mir-210 regulates normoxic gene expression involved in tumor initiation. *Mol. Cell* **35,** 856–867
6. Camps, C., Buffa, F. M., Colella, S., Moore, J., Sotiriou, C., Sheldon, H., Harris, A. L., Gleadle, J. M., and Ragoussis, J. (2008) HSA-miR-210 is induced by hypoxia and is an independent prognostic factor in breast cancer. *Clin. Cancer Res.* **14,** 1340–1348
7. Fasanaro, P., D'Alessandra, Y., Di Stefano, V., Melchionna, R., Romani, S., Pompilio, G., Capogrossi, M. C., and Martelli, F. (2008) MicroRNA-210 modulates endothelial cell response to hypoxia and inhibits the receptor tyrosine kinase ligand Ephrin-A3. *J. Biol. Chem.* **283,** 15878–15883
8. Favaro, E., Ramachandran, A., McCormick, R., Gee, H., Blancher, C., Crosby, M., Devlin, C., Blick, C., Buffa, F., Li, J. L., Vojnovic, B., Pires das Neves, R., Glazer, P., Iborra, F., Ivan, M., Ragoussis, J., and Harris, A. L. (2010) MicroRNA-210 regulates mitochondrial free radical response to

hypoxia and Krebs cycle in cancer cells by targeting iron sulfur cluster protein ISCU. *PLoS ONE* **5,** e10345
9. Puisségur, M. P., Mazure, N. M., Bertero, T., Pradelli, L., Grosso, S., Robbe-Sermesant, K., Maurin, T., Lebrigand, K., Cardinaud, B., Hofman, V., Fourre, S., Magnone, V., Ricci, J. E., Pouysségur, J., Gounon, P., Hofman, P., Barbry, P., and Mari, B. (2011) miR-210 is overexpressed in late stages of lung cancer and mediates mitochondrial alterations associated with modulation of HIF-1 activity. *Cell Death Differ.* **18,** 465–478
10. Zhang, Z., Sun, H., Dai, H., Walsh, R. M., Imakura, M., Schelter, J., Burchard, J., Dai, X., Chang, A. N., Diaz, R. L., Marszalek, J. R., Bartz, S. R., Carleton, M., Cleary, M. A., Linsley, P. S., and Grandori, C. (2009) MicroRNA miR-210 modulates cellular response to hypoxia through the MYC antagonist MNT. *Cell Cycle* **8,** 2756–2768
11. Chan, Y. C., Banerjee, J., Choi, S. Y., and Sen, C. K. (2011) miR-210. The master hypoxamir. *Microcirculation* **19,** 215–223
12. Fasanaro, P., Greco, S., Lorenzi, M., Pescatori, M., Brioschi, M., Kulshreshtha, R., Banfi, C., Stubbs, A., Calin, G. A., Ivan, M., Capogrossi, M. C., and Martelli, F. (2009) An integrated approach for experimental target identification of hypoxia-induced miR-210. *J. Biol. Chem.* **284,** 35134–35143
13. Kosaka, N., Sugiura, K., Yamamoto, Y., Yoshioka, Y., Miyazaki, H., Komatsu, N., Ochiya, T., and Kato, T. (2008) Identification of erythropoietin-induced microRNAs in haematopoietic cells during erythroid differentiation. *Br. J. Haematol.* **142,** 293–300
14. Yang, W., Sun, T., Cao, J., Liu, F., Tian, Y., and Zhu, W. (2012) Downregulation of miR-210 expression inhibits proliferation, induces apoptosis and enhances radiosensitivity in hypoxic human hepatoma cells *in vitro*. *Exp. Cell Res.* **318,** 944–954
15. Gou, D., Ramchandran, R., Peng, X., Yao, L., Kang, K., Sarkar, J., Wang, Z., Zhou, G., and Raj, J. U. (2012) miR-210 has an anti-apoptotic effect in pulmonary artery smooth muscle cells during hypoxia. *Am. J. Physiol. Lung Cell Mol. Physiol.*, L682–L691
16. Quero, L., Dubois, L., Lieuwes, N. G., Hennequin, C., and Lambin, P. (2011) miR-210 as a marker of chronic hypoxia, but not a therapeutic target in prostate cancer. *Radiother. Oncol.* **101,** 203–208
17. Kim, H. W., Haider, H. K., Jiang, S., and Ashraf, M. (2009) Ischemic preconditioning augments survival of stem cells via miR-210 expression by targeting caspase-8-associated protein 2. *J. Biol. Chem.* **284,** 33161–33168
18. Hu, S., Huang, M., Li, Z., Jia, F., Ghosh, Z., Lijkwan, M. A., Fasanaro, P., Sun, N., Wang, X., Martelli, F., Robbins, R. C., and Wu, J. C. (2010) MicroRNA-210 as a novel therapy for treatment of ischemic heart disease. *Circulation* **122,** S124–131
19. Mutharasan, R. K., Nagpal, V., Ichikawa, Y., and Ardehali, H. (2011) microRNA-210 is upregulated in hypoxic cardiomyocytes through Akt- and p53-dependent pathways and exerts cytoprotective effects. *Am. J. Physiol. Heart Circ. Physiol.* **301,** H1519–1530
20. Chan, S. Y., Zhang, Y. Y., Hemann, C., Mahoney, C. E., Zweier, J. L., and Loscalzo, J. (2009) MicroRNA-210 controls mitochondrial metabolism during hypoxia by repressing the iron-sulfur cluster assembly proteins ISCU1/2. *Cell Metab.* **10,** 273–284
21. Yoshioka, Y., Kosaka, N., Ochiya, T., and Kato, T. (2012) Micromanaging iron homeostasis. Hypoxia-inducible miR-210 suppresses iron homeostasis-related proteins. *J. Biol. Chem.* **287,** 34110–34119
22. Chen, Z., Li, Y., Zhang, H., Huang, P., and Luthra, R. (2010) Hypoxia-regulated microRNA-210 modulates mitochondrial function and decreases ISCU and COX10 expression. *Oncogene* **29,** 4362–4368
23. Liu, F., Lou, Y. L., Wu, J., Ruan, Q. F., Xie, A., Guo, F., Cui, S. P., Deng, Z. F., and Wang, Y. (2012) Upregulation of MicroRNA-210 regulates renal angiogenesis mediated by activation of VEGF signaling pathway under ischemia/perfusion injury *in vivo and in vitro*. *Kidney Blood Press. Res.* **35,** 182–191
24. Lou, Y. L., Guo, F., Liu, F., Gao, F. L., Zhang, P. Q., Niu, X., Guo, S. C., Yin, J. H., Wang, Y., and Deng, Z. F. (2012) miR-210 activates notch signaling pathway in angiogenesis induced by cerebral ischemia. *Mol. Cell Biochem.* **370,** 45–51
25. Alaiti, M. A., Ishikawa, M., Masuda, H., Simon, D. I., Jain, M. K., Asahara, T., and Costa, M. A. (2012) Up-regulation of miR-210 by vascular endothelial growth factor in *ex vivo* expanded CD34+ cells enhances cell-mediated angiogenesis. *J. Cell Mol. Med.* **16,** 2413–2421
26. Bianchi, N., Zuccato, C., Lampronti, I., Borgatti, M., and Gambari, R. (2009) Expression of miR-210 during erythroid differentiation and induction of γ-globin gene expression. *BMB Rep.* **42,** 493–499
27. Mizuno, Y., Tokuzawa, Y., Ninomiya, Y., Yagi, K., Yatsuka-Kanesaki, Y., Suda, T., Fukuda, T., Katagiri, T., Kondoh, Y., Amemiya, T., Tashiro, H., and Okazaki, Y. (2009) miR-210 promotes osteoblastic differentiation through inhibition of AcvR1b. *FEBS Lett.* **583,** 2263–2268
28. Qin, L., Chen, Y., Niu, Y., Chen, W., Wang, Q., Xiao, S., Li, A., Xie, Y., Li, J., Zhao, X., He, Z., and Mo, D. (2010) A deep investigation into the adipogenesis mechanism. Profile of microRNAs regulating adipogenesis by modulating the canonical Wnt/β-catenin signaling pathway. *BMC Genomics* **11,** 320
29. Greco, S., Fasanaro, P., Castelvecchio, S., D'Alessandra, Y., Arcelli, D., Di Donato, M., Malavazos, A., Capogrossi, M. C., Menicanti, L., and Martelli, F. (2012) MicroRNA dysregulation in diabetic ischemic heart failure patients. *Diabetes* **61,** 1633–1641
30. Martelli, F., Cenciarelli, C., Santarelli, G., Polikar, B., Felsani, A., and Caruso, M. (1994) MyoD induces retinoblastoma gene expression during myogenic differentiation. *Oncogene* **9,** 3579–3590
31. Cardinali, B., Castellani, L., Fasanaro, P., Basso, A., Alemà, S., Martelli, F., and Falcone, G. (2009) Microrna-221 and microrna-222 modulate differentiation and maturation of skeletal muscle cells. *PLoS ONE* **4,** e7607
32. Zaccagnini, G., Martelli, F., Magenta, A., Cencioni, C., Fasanaro, P., Nicoletti, C., Biglioli, P., Pelicci, P. G., and Capogrossi, M. C. (2007) p66(ShcA) and oxidative stress modulate myogenic differentiation and skeletal muscle regeneration after hind limb ischemia. *J. Biol. Chem.* **282,** 31453–31459
33. Travaglione, S., Messina, G., Fabbri, A., Falzano, L., Giammarioli, A. M., Grossi, M., Rufini, S., and Fiorentini, C. (2005) Cytotoxic necrotizing factor 1 hinders skeletal muscle differentiation *in vitro* by perturbing the activation/deactivation balance of Rho GTPases. *Cell Death Differ.* **12,** 78–86
34. Fasanaro, P., Romani, S., Voellenkle, C., Maimone, B., Capogrossi, M. C., and Martelli, F. (2012) ROD1 is a seedless target gene of hypoxia-induced miR-210. *PLoS ONE* **7,** e44651
35. Gurtner, C., Tu, E., Jamshidi, N., Haigis, R. W., Onofrey, T. J., Edman, C. F., Sosnowski, R., Wallace, B., and Heller, M. J. (2002) Microelectronic array devices and techniques for electric field enhanced DNA hybridization in low-conductance buffers. *Electrophoresis* **23,** 1543–1550
36. Musarò, A., Giacinti, C., Borsellino, G., Dobrowolny, G., Pelosi, L., Cairns, L., Ottolenghi, S., Cossu, G., Bernardi, G., Battistini, L., Molinaro, M., and Rosenthal, N. (2004) Stem cell-mediated muscle regeneration is enhanced by local isoform of insulin-like growth factor 1. *Proc. Natl. Acad. Sci. U.S.A.* **101,** 1206–1210
37. Ono, Y., Sensui, H., Sakamoto, Y., and Nagatomi, R. (2006) Knockdown of hypoxia-inducible factor-1α by siRNA inhibits C2C12 myoblast differentiation. *J. Cell. Biochem.* **98,** 642–649
38. Mason, S. D., Howlett, R. A., Kim, M. J., Olfert, I. M., Hogan, M. C., McNulty, W., Hickey, R. P., Wagner, P. D., Kahn, C. R., Giordano, F. J., and Johnson, R. S. (2004) Loss of skeletal muscle HIF-1α results in altered exercise endurance. *PLoS Biol.* **2,** e288
39. Pisani, D. F., and Dechesne, C. A. (2005) Skeletal muscle HIF-1α expression is dependent on muscle fiber type. *J. Gen. Physiol.* **126,** 173–178
40. Stroka, D. M., Burkhardt, T., Desbaillets, I., Wenger, R. H., Neil, D. A., Bauer, C., Gassmann, M., and Candinas, D. (2001) HIF-1 is expressed in normoxic tissue and displays an organ-specific regulation under systemic hypoxia. *FASEB J.* **15,** 2445–2453
41. Du, Y., Liu, Z., Gu, L., Zhou, J., Zhu, B. D., Ji, J., and Deng, D. (2012) Characterization of human gastric carcinoma-related methylation of 9 miR CpG islands and repression of their expressions *in vitro* and *in vivo*. *BMC Cancer* **12,** 249
42. Scatena, R. (2012) Mitochondria and drugs. *Adv. Exp. Med. Biol.* **942,** 329–346
43. Guzy, R. D., and Schumacker, P. T. (2006) Oxygen sensing by mitochondria at complex III. The paradox of increased reactive oxygen species during hypoxia. *Exp. Physiol.* **91,** 807–819
44. d'Albis, A., Couteaux, R., Janmot, C., Roulet, A., and Mira, J. C. (1988)

Regeneration after cardiotoxin injury of innervated and denervated slow and fast muscles of mammals. Myosin isoform analysis. *Eur. J. Biochem.* **174,** 103–110
45. Tsuchiya, S., Oku, M., Imanaka, Y., Kunimoto, R., Okuno, Y., Terasawa, K., Sato, F., Tsujimoto, G., and Shimizu, K. (2009) MicroRNA-338–3p and microRNA-451 contribute to the formation of basolateral polarity in epithelial cells. *Nucleic Acids Res.* **37,** 3821–3827
46. Hildebrand, J., Rütze, M., Walz, N., Gallinat, S., Wenck, H., Deppert, W., Grundhoff, A., and Knott, A. (2011) A comprehensive analysis of microRNA expression during human keratinocyte differentiation *in vitro* and *in vivo*. *J. Invest Dermatol.* **131,** 20–29
47. Kane, N. M., Meloni, M., Spencer, H. L., Craig, M. A., Strehl, R., Milligan, G., Houslay, M. D., Mountford, J. C., Emanueli, C., and Baker, A. H. (2010) Derivation of endothelial cells from human embryonic stem cells by directed differentiation. Analysis of microRNA and angiogenesis *in vitro* and *in vivo*. *Arterioscler. Thromb. Vasc. Biol.* **30,** 1389–1397
48. Zhang, Y., Fei, M., Xue, G., Zhou, Q., Jia, Y., Li, L., Xin, H., and Sun, S. (2012) Elevated levels of hypoxia-inducible microRNA-210 in pre-eclampsia. New insights into molecular mechanisms for the disease. *J. Cell Mol. Med.* **16,** 249–259
49. Guttridge, D. C., Albanese, C., Reuther, J. Y., Pestell, R. G., and Baldwin, A. S., Jr. (1999) NF-κB controls cell growth and differentiation through transcriptional regulation of cyclin D1. *Mol. Cell. Biol.* **19,** 5785–5799
50. Milkiewicz, M., Pugh, C. W., and Egginton, S. (2004) Inhibition of endogenous HIF inactivation induces angiogenesis in ischaemic skeletal muscles of mice. *J. Physiol.* **560,** 21–26
51. Bloomer, R. J., and Goldfarb, A. H. (2004) Anaerobic exercise and oxidative stress. A review. *Can J. Appl. Physiol.* **29,** 245–263
52. Musarò, A., Fulle, S., and Fanò, G. (2010) Oxidative stress and muscle homeostasis. *Curr. Opin Clin. Nutr. Metab. Care* **13,** 236–242
53. Kon, M., Tanabe, K., Lee, H., Kimura, F., Akimoto, T., and Kono, I. (2007) Eccentric muscle contractions induce greater oxidative stress than concentric contractions in skeletal muscle. *Appl Physiol. Nutr. Metab.* **32,** 273–281